

Biot's Consolidation analysis using the node-based smoothed point interpolation method (NS-PIM)

Shiyang Pan¹, Tongchun Li¹, †Jing Cheng^{1,2}, Ping Yuan³, and Xinyang Ning¹

¹ College of Water Conservancy and Hydropower Engineering, Hohai University, Nanjing 210098, Peoples Republic of China

² 210 KAP Hall, University of Southern California, Los Angeles, CA 90089, U.S.A

³ Zhongye Changtian International Engineering Co., Ltd, Changsha 410007, Peoples Republic of China

†Corresponding author: mscj042@hotmail.com.

ABSTRACT

The node-based smoothed point interpolation method (NS-PIM) is developed for soil consolidation analysis based on the Biot's theory. Both the shape functions for displacements and pore pressures are constructed using the point interpolation method which is easier to be programmed than the other meshless methods. Then, a 2D consolidation problem under ramp load is solved. The results show good agreement with those certified results. Meanwhile, convergence features of different solutions are studied and useful convergence features are found. Thus a simple method is introduced to estimate the errors of the model with rough grids. Obviously, it is promising to apply NS-PIM to the analysis of consolidation problems.

Keywords: Meshless Methods, NS-PIM, Consolidation, Biot's theory, FEM

1 INTRODUCTION

Consolidation analysis is necessary in many situations such as foundation settlement analysis, earth and rock fill dam analysis and so on.[1][2] Generally, the consolidation analysis in one dimensional field is based on the Terzaghi theory[3] in soil mechanics, while the Biot's consolidation theory[4][5] is usually applied in two dimensional and three dimensional fields.

The finite element method[6] has been developed to solve lots of problems and great achievements has been made[7]. With the development of finite element method and the improvement of computer performance, numerous programs using the Biot's theory based on the finite element method have been developed to solve practical problems in consolidation analysis. Those programs using the finite element method are relatively easy to be programmed and the results can be checked in many commercial soft wares and monographs[8]. However, the building and mesh of models takes place of most of the time for the analysis of FEM solution. Many mistakes may also take place during the building of the models. And it is also hard to get accurate results, unless the dense of the grid is sufficient.

Thus, the mesh-free(or meshless) method[9] was put forward to deal with the problems mentioned above. And there are many kinds of element-free or mesh-free methods, such as reproducing kernel particle method (RKPM), HP-cloud method, point interpolation method (PIM) and so on. The node-based smoothed point interpolation method (NS-PIM or LC-PIM) [10][11], as one of the mesh free methods, has been developed using the node-based strain smoothing operation[12]. Formulated by polynomial PIM [13] or radial PIM (RPIM) [14] shape functions, it possesses the Kronecker delta property and the boundary can be enforced like that of the FEM solution[15], so that the programming of the NS-PIM can be easier than the programming of many other mesh free methods.

It has been certified that the NS-PIM and FEM solutions possess different convergence features[16][17]. And it is significant to apply the NS-PIM solution to consolidation problem in order to get more accurate results with the comparison to those by the FEM solution[18]. Also, the adaptability of mesh free methods to large deformation as the shape functions are based on nodes is meaningful for consolidation problems like foundation settlement.

Recent years, some PIM programs for elastic problem and consolidation problem[19] have been developed, but NS-PIM solution is rarely applied to consolidation problems. With all the features mentioned above, it is meaningful and necessary to apply NS-PIM to the analysis of consolidation problems and do some further research.

In this work, the node-based smoothed point interpolation method(NS-PIM) is built and coded for Biot's consolidation analysis. Then, the NS-PIM solution is applied to a classic example to check the correctness and validation together with the FEM solution. It is confirmed that the results of the NS-PIM solution fit well with the certified FEM results. So that it is feasible to apply the NS-PIM solution to the Biot's consolidation analysis. Further more, different mesh schemes are applied to investigate the convergence features of different solutions. The investigation shows that the NS-PIM and FEM solutions still possess the certified convergence features which can be used as a method to get more accurate results. So that a simple method is introduced to estimate the errors of the results with rough grids.

2 BRIEFING ON FORMULATIONS AND SHAPE FUNCTIONS

Some basic formulations and shape functions for NS-PIM are introduced in this part. The programming of the solution is also introduced.

2.1 Basic equations for Biot's theory

The basic theory used to write the NS-PIM program is the Biot's consolidation theory .

On the one hand, the sets of partial differential equations for two dimensional equilibrium in consolidation problems are listed as follows :

$$\begin{aligned}\frac{\partial \sigma'_x}{\partial x} + \frac{\partial \tau_{xy}}{\partial y} + \frac{\partial u_w}{\partial x} &= f_x \\ \frac{\partial \tau_{xy}}{\partial x} + \frac{\partial \sigma'_y}{\partial y} + \frac{\partial u_w}{\partial y} &= f_y\end{aligned}\tag{1}$$

where u_w is the excess pore pressure , τ_{xy} is the shearing stress , $f_x f_y$ are the forces in x- , y- directions and σ'_x, σ'_y are the effective stresses.

$$\{\sigma'\} = [D]\{\varepsilon\}\tag{2}$$

where $[D]$ is the constitutive matrix and $\{\varepsilon\}$ is the strain matrix.

In linear elastic problem, the constitutive matrix $[D]$ is an elastic matrix. Then,

$$\begin{aligned}\sigma'_x &= \frac{E'}{(1+\nu')} \left(\frac{\nu'}{(1-2\nu')} \varepsilon_v + \varepsilon_x \right) \\ \sigma'_y &= \frac{E'}{(1+\nu')} \left(\frac{\nu'}{(1-2\nu')} \varepsilon_v + \varepsilon_y \right) \\ \tau_{xy} &= \frac{E'}{2(1+\nu')} \gamma_{xy}\end{aligned}\tag{3}$$

where ε_v is the volumetric strain, $\varepsilon_x \varepsilon_y$ are the x- y- strain, γ_{xy} is the shearing strain, E' is the effective Young's modulus and ν' is the poisson's ratio.

Further more, assuming small strains , the geometric equation is

$$\{\varepsilon\} = [\partial]\{u\}\tag{4}$$

where $\{\varepsilon\}$ is the strain matrix , $\{u\}$ is the displacement matrix and $[\partial]$ is the partial differential operator matrix .

Thus, equation (1) can be rewritten as follows:

$$\begin{aligned} \frac{E'(1-\nu')}{(1+\nu')(1-2\nu')} \left[\frac{\partial^2 u_x}{\partial x^2} + \frac{(1-2\nu')}{2(1-\nu')} \frac{\partial^2 u_x}{\partial y^2} + \frac{1}{2(1-\nu')} \frac{\partial^2 u_y}{\partial x \partial y} \right] + \frac{\partial u_w}{\partial x} &= f_x \\ \frac{E'(1-\nu')}{(1+\nu')(1-2\nu')} \left[\frac{1}{2(1-\nu')} \frac{\partial^2 u_x}{\partial x \partial y} + \frac{\partial^2 u_y}{\partial y^2} + \frac{(1-2\nu')}{2(1-\nu')} \frac{\partial^2 u_y}{\partial x^2} \right] + \frac{\partial u_w}{\partial y} &= f_y \end{aligned} \quad (5)$$

where u_x is the x-displacement and u_y is the y-displacement .

On the other hand, assuming fluid incompressibility and 2D continuity ,the continuity equation takes the following form :

$$\frac{\partial \varepsilon_v}{\partial t} + \frac{k}{\gamma_w} \nabla^2 u_w = 0 \quad (6)$$

where $\varepsilon_v = \frac{\partial u_x}{\partial x} + \frac{\partial u_y}{\partial y}$ is the volumetric strain , t is the time, k is the matrix of permeabilities in the x- and y-directions , γ_w is the unit weight of water and $\nabla^2 = \frac{\partial^2}{\partial x^2} + \frac{\partial^2}{\partial y^2}$ is the Laplace operator .

Now ,the coupled ‘Biot’ equations for a 2D homogeneous poroelastic material can be listed as follows by combining equations (5) - (6) :

$$\begin{aligned} \frac{E'(1-\nu')}{(1+\nu')(1-2\nu')} \left[\frac{\partial^2 u_x}{\partial x^2} + \frac{(1-2\nu')}{2(1-\nu')} \frac{\partial^2 u_x}{\partial y^2} + \frac{1}{2(1-\nu')} \frac{\partial^2 u_y}{\partial x \partial y} \right] + \frac{\partial u_w}{\partial x} &= f_x \\ \frac{E'(1-\nu')}{(1+\nu')(1-2\nu')} \left[\frac{1}{2(1-\nu')} \frac{\partial^2 u_x}{\partial x \partial y} + \frac{\partial^2 u_y}{\partial y^2} + \frac{(1-2\nu')}{2(1-\nu')} \frac{\partial^2 u_y}{\partial x^2} \right] + \frac{\partial u_w}{\partial y} &= f_y \\ \frac{\partial}{\partial t} \left(\frac{\partial u_x}{\partial x} + \frac{\partial u_y}{\partial y} \right) + \frac{k_x}{\gamma_w} \frac{\partial^2 u_w}{\partial x^2} + \frac{k_y}{\gamma_w} \frac{\partial^2 u_w}{\partial y^2} &= 0 \end{aligned} \quad (7)$$

2.2 Discretization of Biot's theory

To solve the set of simultaneous equations in equation (7), the displacement variables u_x, u_y and excess pore pressure u_w need to be discretized in the equations showed as follows ,

$$\begin{aligned} \bar{u}_x &= [N]\{u_x\} \\ \bar{u}_y &= [N]\{u_y\} \\ \bar{u}_w &= [N]\{u_w\} \end{aligned} \quad (8)$$

where \bar{u}_x, \bar{u}_y are the element or nodal displacements in x-, y- directions , \bar{u}_w is the element or nodal excess pore pressure and $[N]$ is the corresponding shape function matrix.

In practice, it may be more appropriate to use higher order shape functions for u_x and u_y to avoid oscillation[20]. But, in this work, all three variables are described by the same order of shape functions which means the solution in this work may have the problem of oscillation under some extreme conditions.

After all the discretization and Galerkin process , equation (7) can be rewritten as follows :

$$\begin{aligned} [k_m]\{u\} + [c]\{u_w\} &= \{f\} \\ [c]^T \left\{ \frac{du}{dt} \right\} - [k_p]\{u_w\} &= \{0\} \end{aligned} \quad (9)$$

where $[k_m]$ is the elastic stiffness matrix , $[k_p]$ is the fluid conductivity matrix and $[c] = \iint \frac{\partial N_i}{\partial x} N_j dx dy$ is the coupling matrix where N_i is the shape function of the displacement filed and N_j is the shape function of the excess pore pressure filed .

The following equations for writing the program can be obtained by integrating Equation (9) in time and doing interpolation using θ , and then Equation (10) can be obtained :

$$\begin{aligned} &\begin{bmatrix} \theta[k_m] & \theta[c] \\ \theta[c]^T & -\theta^2 \Delta t [k_p] \end{bmatrix} \begin{Bmatrix} \{u\} \\ \{u_w\}_1 \end{Bmatrix} \\ &= \begin{bmatrix} -(1-\theta)[k_m] & -(1-\theta)[c] \\ \theta[c]^T & \theta(1-\theta)\Delta t [k_p] \end{bmatrix} \begin{Bmatrix} \{u\} \\ \{u_w\}_0 \end{Bmatrix} + \begin{Bmatrix} (1-\theta)f \\ \{0\} \end{Bmatrix}_0 + \begin{Bmatrix} \theta f \\ \{0\} \end{Bmatrix}_1 \end{aligned} \quad (10)$$

where θ is the time-stepping parameter ($0.5 \leq \theta \leq 1$). To avoid oscillatory results ,the fully implicit method with $\theta = 1$ is used in the NS-PIM solution. In this work, the left side matrix

$\begin{bmatrix} \theta[k_m] & \theta[c] \\ \theta[c]^T & -\theta^2 \Delta t [k_p] \end{bmatrix}$ in Equation (10) is called ‘Kt’ and the right side matrix $\begin{bmatrix} -(1-\theta)[k_m] & -(1-\theta)[c] \\ \theta[c]^T & \theta(1-\theta)\Delta t [k_p] \end{bmatrix}$ is called ‘Kd’. Also, in equation (10)

$$\begin{aligned} k_m &= \iint [B]^T [D][B] dx dy \\ k_p &= \iint [T]^T [K][T] dx dy \end{aligned} \quad (11)$$

where $[B]$ is the strain–displacement matrix , $[D]$ is the stress–strain matrix, $[T]$ is the ‘ $[B]$ matrix’ for fluid and $[K]$ is the ‘ $[D]$ matrix’ for fluid.

2.3 Simulate load in construction period

The load is usually applied step by step in a construction period. To simulate this process, the total load should be divided into several part according to the construction period. The previous load $\{R_{tp}\}$, the current load $\{R_{tc}\}$ and the effective stress $\{R_p\}$ generated by the previous load is needed to calculate the load $\{R_c\}$ for the current time. And

$$\{R_c\} = \{R_{tc}\} + (\{R_{tp}\} - \{R_p\}) \quad (12)$$

This load $\{R_c\}$ would be the external force applied in current time step. Thus, the simulation is realized.

2.4 Shape functions for NS-PIM

Triangular cells are used for the mesh of models, since the triangular cells are more adaptive to complex geometry. Polynomials which are usually built utilizing Pascal triangle are used in the interpolation to create shape functions for NS-PIM. The Figure 1 is the Pascal triangle of which the first two lines are used for complete polynomial basis of first order and the first three lines are used for complete polynomial basis of second order in two-dimensional domain, as is listed below.

$$p^T(x) = \{1 \ x \ y\} \quad (13)$$

$$p^T(x) = \{1 \ x \ y \ x^2 \ xy \ y^2\} \quad (14)$$

where $p^T(x)$ is the complete polynomial basis mentioned above , $x \ y$ are the coordinates of each node.

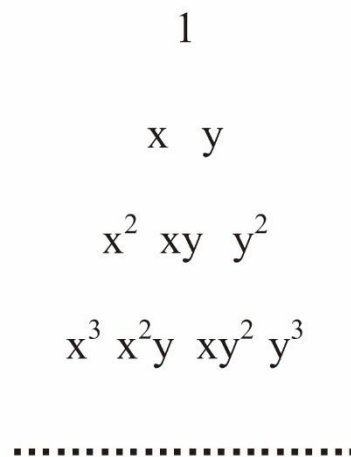


Figure 1. Pascal triangle for two-dimensional domains

The vector of shape functions is

$$\Phi^T(x) = p^T(x)P_n^{-1}(x) = \{\varphi_1 \ \varphi_2 \ \dots \ \varphi_n\} \quad (15)$$

where n is the number of nodes, φ is the shape function of each node, $P_n^{-1}(x)$ is the moment matrix and

$$P_n(x) = \begin{bmatrix} 1 & x_1 & y_1 & x_1 y_1 & \cdots & p_n(x_1) \\ 1 & x_2 & y_2 & x_2 y_2 & \cdots & p_n(x_2) \\ \vdots & \vdots & \vdots & \vdots & \ddots & \vdots \\ 1 & x_n & y_n & x_n y_n & \cdots & p_n(x_n) \end{bmatrix} \quad (16)$$

2.4.1 Supporting nodes for interpolation

For NS-PIM, there are two schemes available to create the needed shape functions, T3-scheme and T6/3-scheme [21]. The T3-scheme is a scheme utilizing the vertexes of each cell to create the shape functions. In the T6/3-scheme, the vertexes of an interior cell that has no edge on the boundary of the problem domain and its neighboring cells sharing one edge with this interior cell are needed to create the shape functions, while the vertexes of a boundary cell that has at least one edge on the boundary are enough to create the corresponding shape functions .

As is showed in Figure 2 , cell 1 (ABD) is a boundary cell and cell 2 (BPD) is an interior cell. Node A, B, D would be enough to create shape functions of cell 1 and cell 2 for the T3-scheme of NS-PIM. However, six nodes (node A, B, D, E, F, P) are needed to create the shape functions of cell 2 for the T6/3-scheme of NS-PIM.

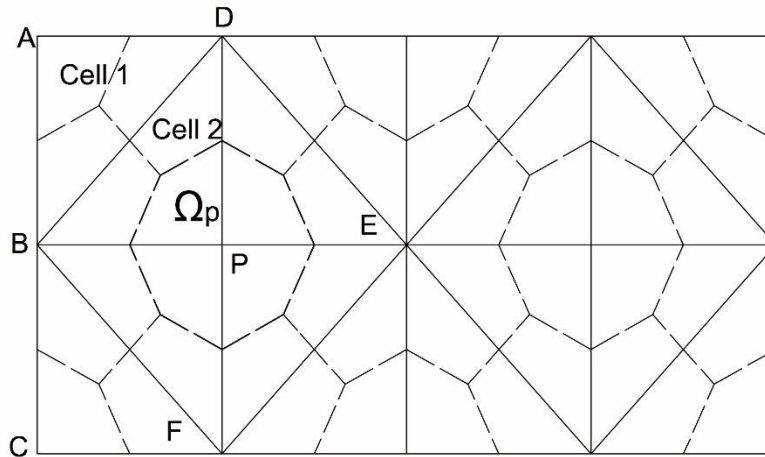


Figure 2. Background cells and the construction of smoothing cells

2.4.2 Integral domain

Shape functions for NS-PIM can be constructed by the nodes attached to the cells. In practice, to ensure the continuity of the shape functions ,the problem domain of NS-PIM needs to be divided into smoothing domains based on background cells [22].

As shown in Figure 2, the solid lines is the lines for the background cells and the smoothing domains are constructed by the dotted lines that is connecting the mid-edge-point to the centroids of the cells. For example, in Figure 2 ,the sub-domain Ω_p is the domain for the point P.

2.5 Programming of the NS-PIM solution

The consolidation analysis program for NS-PIM solution is based on the Fortran90 language and applicable for linear elastic Biot's consolidation analysis.

The programming of the NS-PIM solution is best explained by the flowchart of Figure 3. There are two main loops in this program: node-looping and time-looping. Many global matrices of equation (10) are formed in the node-looping and the results of each loading step can be obtained in the time-looping. **Table I** is the list of some main subroutines and their functions.

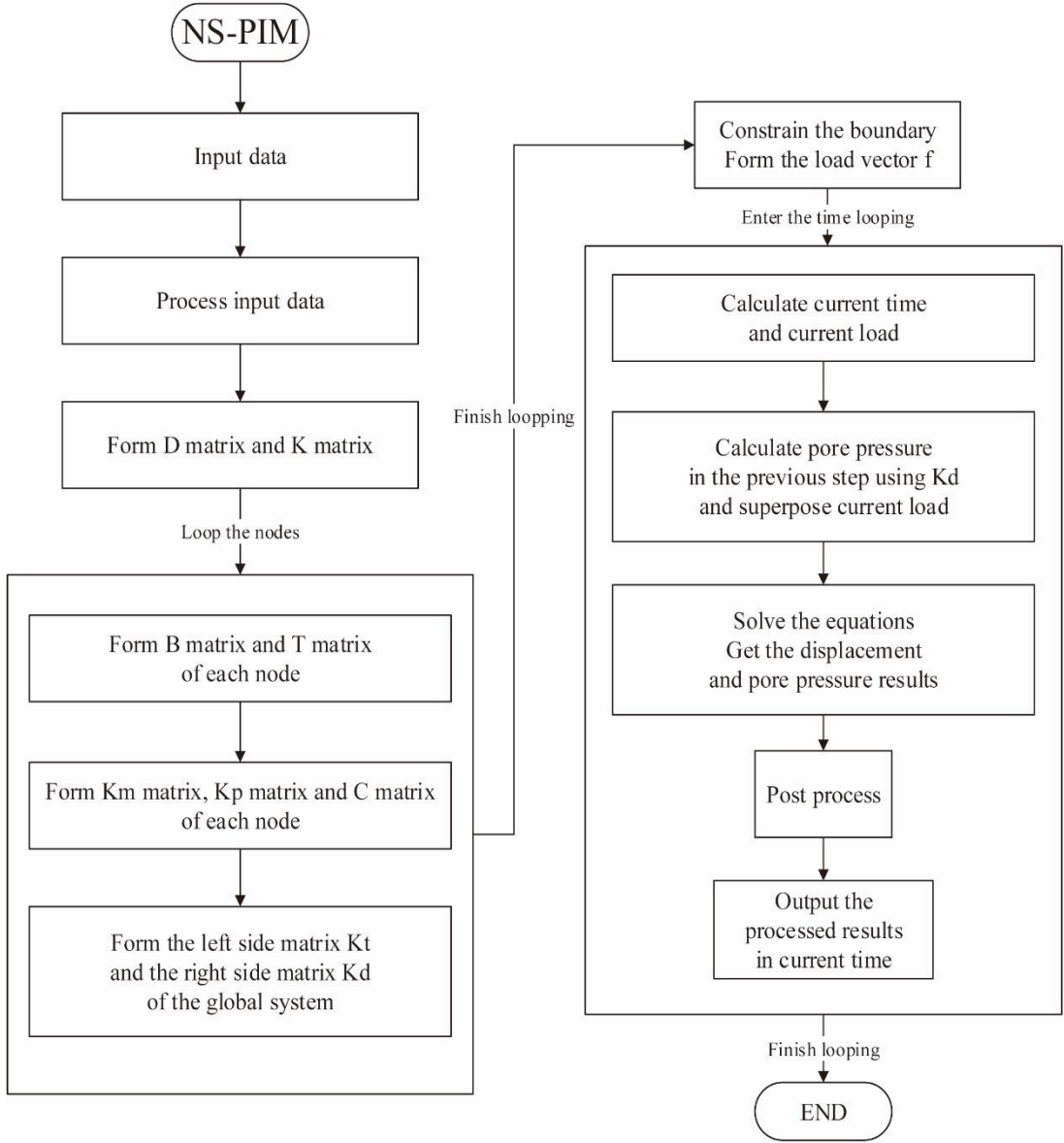


Figure 3. Flowchart of NS-PIM program

Table I. Main subroutines and functions

Subroutine Name	Function
D_Form, K_Form	Form the D matrix and K matrix
FormBCT	Form the B T and C matrices of each node
Stiff_point_Km, Stiff_point_Kp	Form the Km and Kp matrices of each node
Stiff_point_KN	Form the left side matrix of each node
Stiff_point_KD	Form the right side matrix of each node
Form_BG	Form the global left side matrix
Form_Pb	Form the global right side matrix
Traction	Form the total load vector
EBCs	Constrain the boundary
EquaSolvBand	Solve the equations
Tecout_mult	Output the results

3 NUMERICAL EXAMPLES

Firstly, a classic 2D Biot elastic solid example is applied to certify the correctness and validation of the PIM solution and T3-scheme is applied to create the shape functions for NS-PIM. Then, the mesh of the same model is refined to investigate the convergence feature of the NS-PIM and FEM solutions.

3.1 Classic 2D consolidation problem

3.1.1 Model and Material parameters

A classic homogeneous 2D Biot elastic solid example is simulated in this part[8]. For convenience, the permeabilities in the x- and y-directions are considered numerically equal to the unit weight of water which means the effect of Mandal would not be observed easily. Also, the effective Young's modulus and the poisson's ratio is taken respectively as 1 and 0.

A plane strain consolidation model is built in this problem, as shown by the mesh and constraints given in Figure 4. The width and depth of the model is 1m and 10m. The base and sides of the mesh are impermeable boundaries and both restrained in the normal direction of the boundaries. The top of the model is drained, and subjected to the ramp loading shown in Figure 5 ,which indicates a linearly increasing load reaching a maximum of 1.0 at time t_0 . In this case, there are ten load steps, twenty time steps, and the duration of each step is one second.

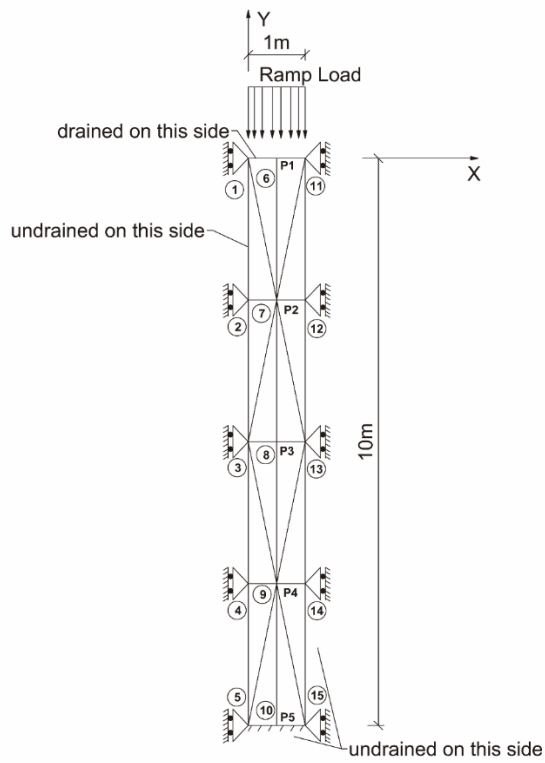


Figure 4. Mesh and constraints of the 2D Biot elastic solid model

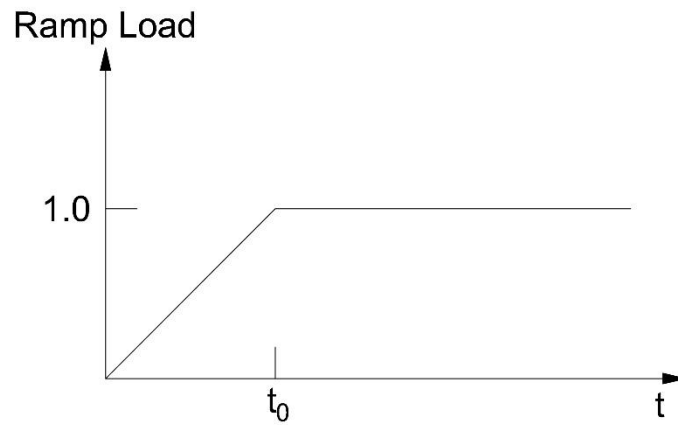


Figure 5. Ramp loading

3.1.2 Distributions of the results

The distributions of Y-displacement and pore pressure results using NS-PIM solution are calculated and the results of step 1, step 5, step 10, step 11, step 15 and step 20 are shown in Figure 6 and Figure 7.

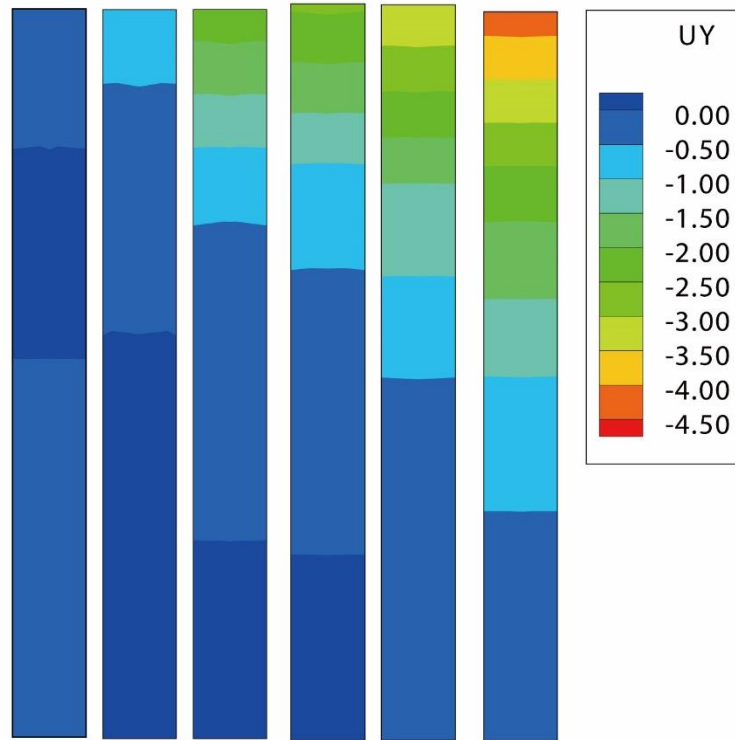


Figure 6 Distributions of Y-Displacement by NS-PIM(T3) in different steps (mm)

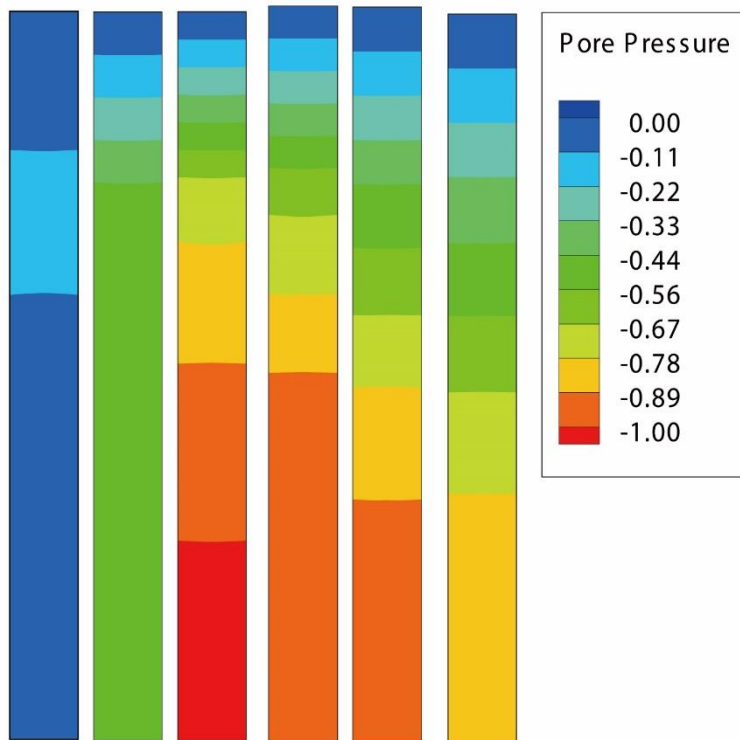


Figure 7 Distributions of pore pressure by NS-PIM(T3) in different steps (Pa)

Extracting the Y-displacement of different steps from top to bottom ('P1'-'P5') to plot a graph of the distribution of Y-displacement by different solutions as is showed in Figure 8 and Figure 9.

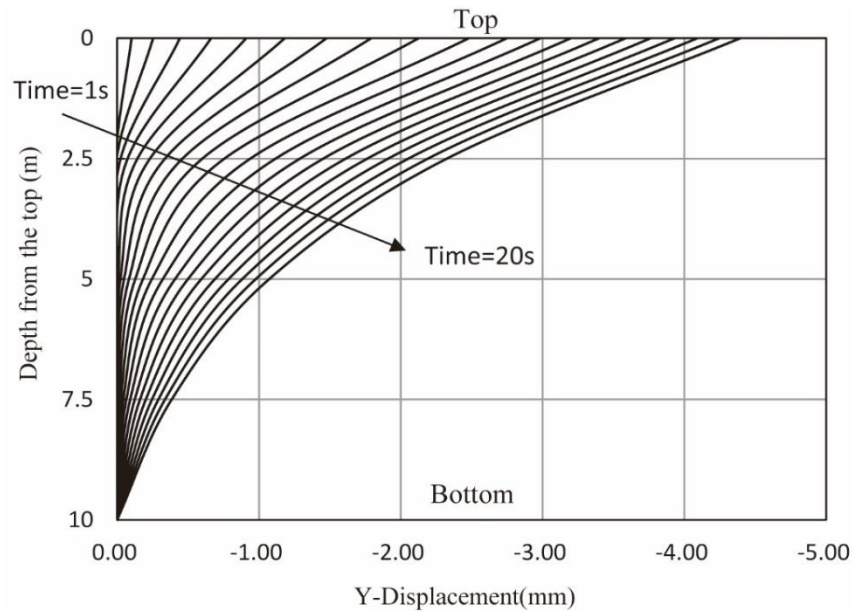


Figure 8 Distributions of Y-Displacement at different times by NS-PIM(T3)

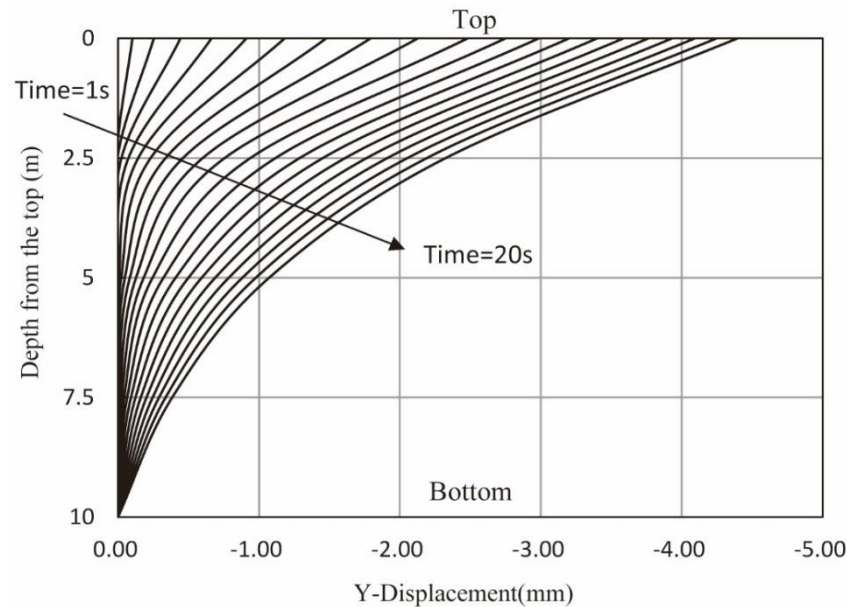


Figure 9 Distributions of Y-Displacement at different time by FEM

As is described in the figures above, the Y-displacement values by both solutions increase gradually from bottom to top, while the pore pressure values increase gradually from top to bottom. Also, the Y-displacement values at each point keep increasing, while the pore pressure values first increase then decrease with the increase of time. Comparing with the general rules, the distributions of the results obtained by both the FEM solution and the NS-PIM solution described above are reasonable.

3.1.3 Time history of the results

In order to study the time-dependent change of the results obtained by NS-PIM, five points from top to bottom ('P1'-'P5') in the middle of the model are selected to plot the time series graphs of the Y-Displacement results and pore pressure results. The graphs are shown in Figure 10 and Figure 11.

To take a close investigation of different solutions, combining the displacement values of 'P1' and the pore pressure values of 'P5' by NS-PIM and FEM. The graphs are shown in Figure 12 and Figure 13.

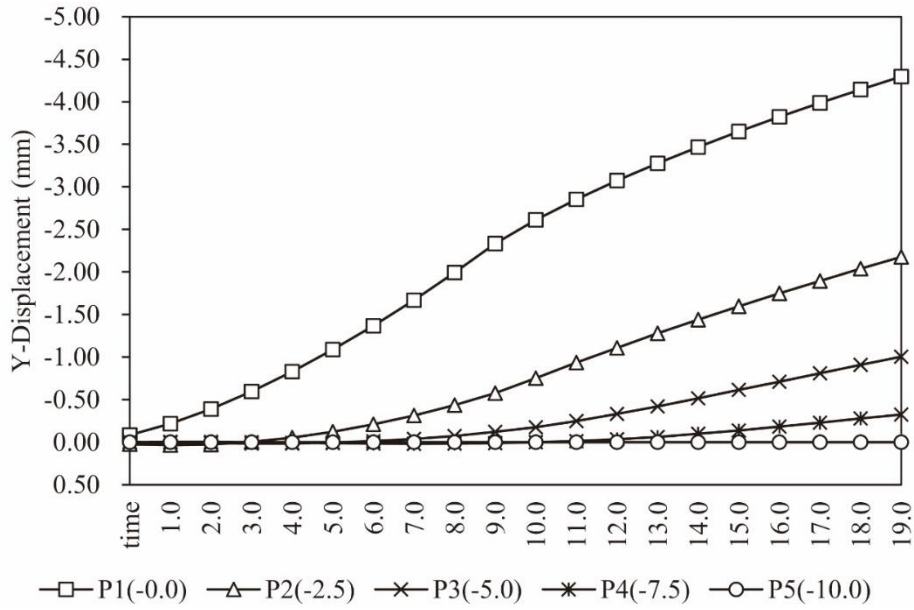


Figure 10 Time series graph of the Y-Displacement results by NS-PIM(T3) (mm)

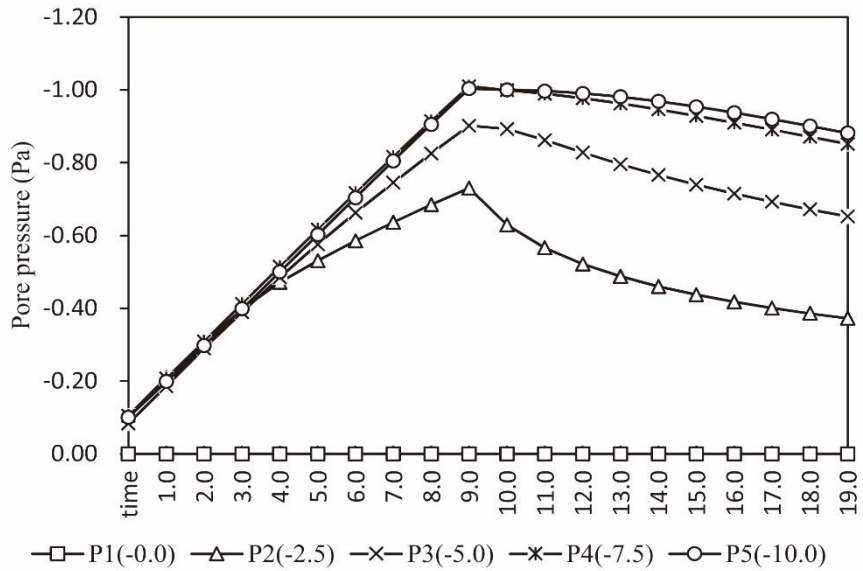


Figure 11 Time series graph of the pore pressure results by NS-PIM(T3) (Pa)

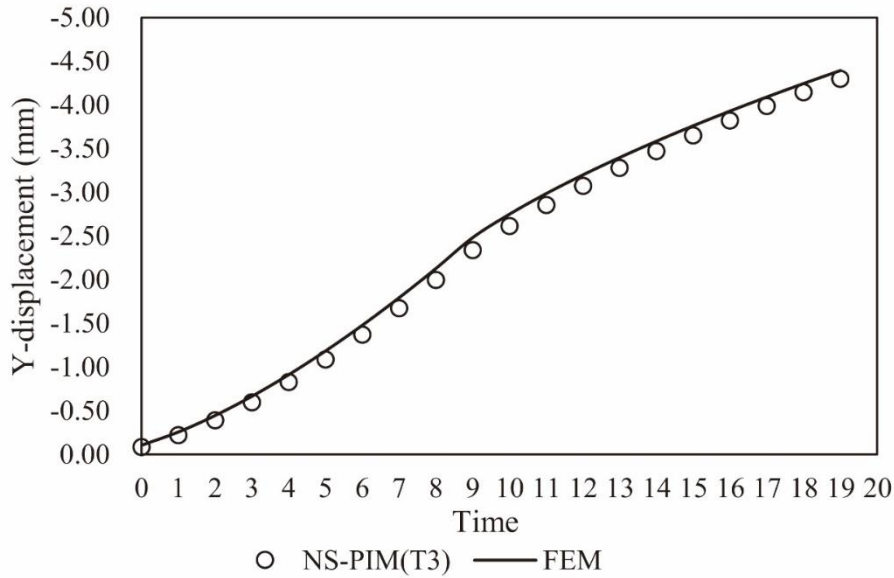


Figure 12 The Y-displacement values of ‘P1’ by different solutions(mm)

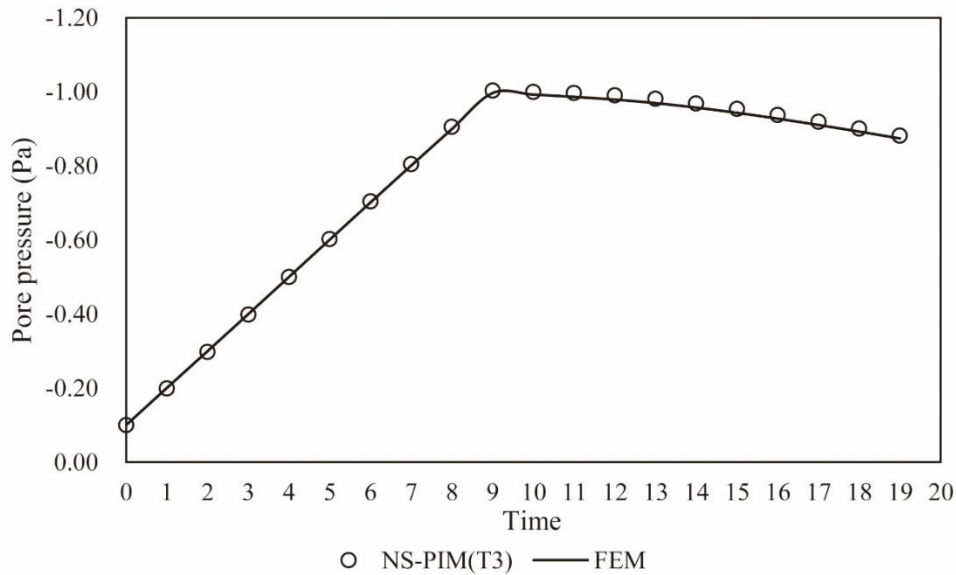


Figure 13 The Pore pressure values of ‘P5’ by different solutions(Pa)

The relations between the results and time is well simulated by NS-PIM, that is the Y-Displacement values increase gradually over time and the pore pressure values first increase then decrease with the increase of time. Also, the results are equivalent to those of the FEM solution. However, the time series curve in Figure 11 is a little abnormal during the time from 0s to 4s, and this is considered to be the computational error of the NS-PIM program.

Although the distributions and time series graphs of NS-PIM and FEM solutions share the similar rules as is described above, there are still some differences between the results of two solutions which can be found from careful comparison. Thus, it is necessary to compare the results with those of the certified results in Schiffman RL’s report(1960) [8,23] to confirm the correctness and validation of the NS-PIM solution.

3.1.4 Certification of the results

In order to compare the calculated results in this example with the certified results in Schiffman RL's report(1960), the time of the simulation is extended to 1000 seconds. Also, the dimensionless 'time factor' T is defined as

$$T = \frac{c_v t}{D^2} \quad (17)$$

Where D is the 'maximum drainage path'(depth) of the model, t is the time of the simulation and c_v is the coefficient of consolidation. c_v is defined as

$$c_v = \frac{k_y}{m_v \gamma_w} \quad (18)$$

where k_y is the permeability in the y-direction, γ_w is the unit weight of water and m_v is defined as

$$m_v = \frac{(1 - \nu')(1 - 2\nu')}{E'(1 - \nu')} \quad (19)$$

where E' is the effective Young's modulus and ν' is the poisson's ratio.

At the beginning of this part ,it is mentioned that D is 10m, k_y equals to γ_w , E' is 1 and ν' is 0. Thus, the dimensionless 'time factor' T equals to 0.01t, and the pore pressure of different solutions at the base of the mesh (P5) is plotted against time in Figure 14 .

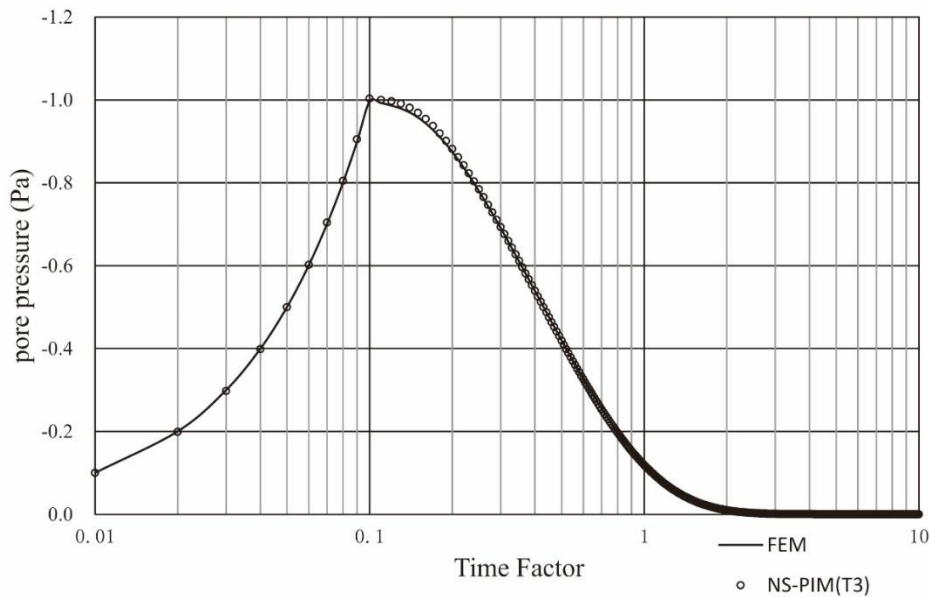


Figure 14 Pore pressure response to ramp loading at 'P5' by different solutions

As is described in the figures above, the pore pressures of both solutions rises to peak(1.0Pa) till the time factor is 0.1, then the pore pressure decreases slowly to zero. Comparing the figures above with the corresponding figures in Schiffman RL's report (1960)[23], conclusions can be drawn that the results calculated by both solutions are correct and valid.

3.1.5 Mesh refinement

Further research is carried out in order to study the convergence features of the NS-PIM solution. The same model as Figure 4 is created in this part. Main parameters are also listed in part 3.1.1 .

The Figure 15 is the same model using different mesh schemes. Details of the models and the results calculated by the NS-PIM and FEM solutions in the 20th time step(last time step of the analysis) are listed in Table II . Figure 16 and Figure 17 are the logarithmic graphs of the maximum Y-Displacement and maximum pore pressure in the 20th time step which indicate that the results of both solutions possess good convergency .

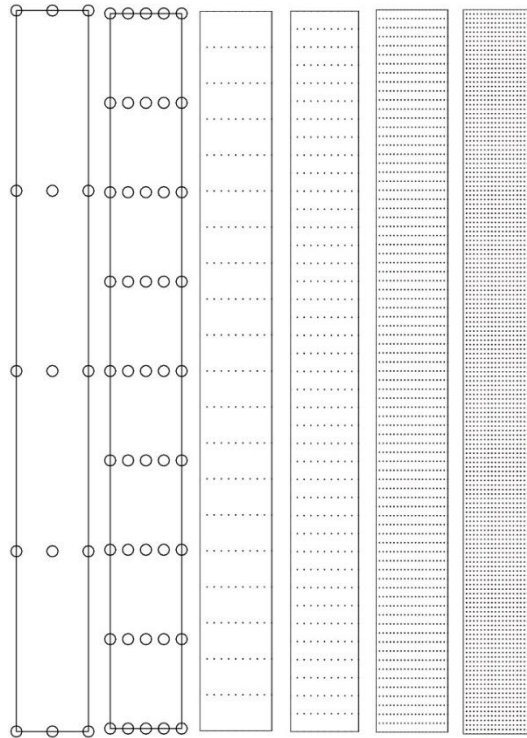
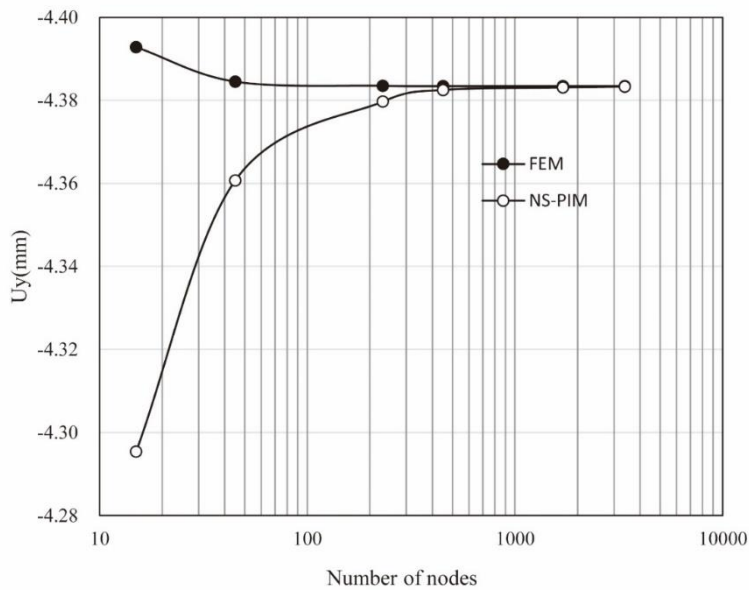


Figure 15 Six different mesh schemes

Table II. Results of different mesh schemes

Mesh Scheme	1	2	3	4	5	6
Number of nodes	15	45	231	451	1701	3381
Number of cells	16	64	400	800	3200	6400
Maximum Y-Displacement in the 20th time step (NS-PIM(T3))	-4.29540	-4.36070	-4.37970	-4.38250	-4.38310	-4.38330
Maximum Pore pressure in the 20th time step (NS-PIM(T3))	-0.88144	-0.85975	-0.85398	-0.85312	-0.85292	-0.85286
Maximum Y-Displacement in the 20th time step (FEM)	-4.39280	-4.38450	-4.38350	-4.38340	-4.38340	-4.38340
Maximum Pore pressure in the 20th time step (FEM)	-0.87418	-0.85822	-0.85369	-0.85305	-0.85289	-0.85285

**Figure 16 Maximum Y-Displacement in the 20th time step by FEM and NS-PIM**

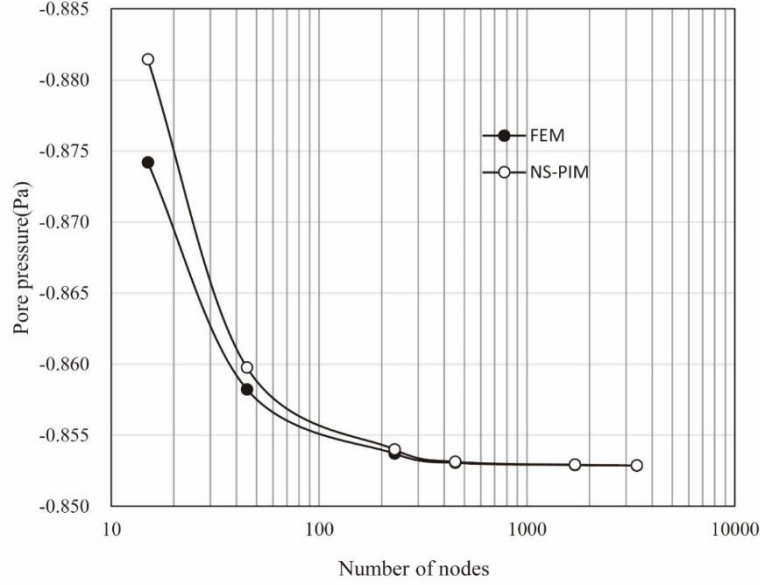


Figure 17 Maximum pore pressure in the 20th time step by FEM and NS-PIM

The graphs of Figure 16 and Figure 17 indicate that the calculated displacement values of NS-PIM and FEM solutions converge towards the exact values from different sides, while the calculated pore pressure values of both solutions converge towards the exact values from the same side. Thus, more accurate results and computational error can be obtained by comparing the results calculated by the NS-PIM and FEM solutions.

3.1.6 Error Estimation

Based on the convergence features of the NS-PIM and FEM, equation (20) and equation (21) is defined to estimate the errors of the current model.

$$ERR = \frac{|D_{exact} - D_{numer}|}{|D_{exact}|} \quad (20)$$

$$ERR1 = \frac{|D_{NS-PIM} - D_{FEM}|}{\min\{|D_{NS-PIM}|, |D_{FEM}|\}} \quad (21)$$

where ERR is the exact error, $ERR1$ is the calculated error, and D_{exact} , D_{numer} , D_{NS-PIM} , D_{FEM} mean the exact maximum value, maximum value from numerical method, NS-PIM and FEM, respectively.

As regard to the displacement values, it can be seen from Figure 16 that $|D_{NS-PIM} - D_{FEM}| > |D_{NS-PIM} - D_{exact}|$ and $|D_{NS-PIM} - D_{FEM}| > |D_{exact} - D_{FEM}|$, hence $ERR1 > ERR$ which means the $ERR1$ for displacement is an overestimate of ERR .

As for the pore pressure values, the exact value is less than the calculated values by both solutions. But, it still can be found from Figure 17 that the values by both solutions getting closer to each other, while they are approaching the exact value. Thus, Equation (21) can still be used as an estimation of the error.

Take the results of mesh scheme 1 for example, the $ERR1$ for displacement is equal to 2.27% and the $ERR1$ for pore pressure is equal to 0.83%. If the accuracy is enough, mesh scheme 1 would be enough to get the results. Otherwise, finer mesh schemes should be used to get the satisfactory results.

This approach for estimating the calculation error is quite useful, as the estimated error can be obtained with just one set of model and cells which means more time can be saved from the boring work of modeling and remeshing.

4 CONCLUSIONS AND DISCUSSIONS

Node-based smoothed point interpolation method is applied to the Biot's consolidation analysis in this work. Results are compared to those of the certified FEM solution to check the correctness and validation of the NS-PIM solution. Also, a simple method is introduced to estimate the errors of the results with rough grids.

The conclusions of the comparison are listed as follows:

- 1) It is feasible to apply the NS-PIM solution to the Biot's consolidation analysis. And the results of the solution fit well with the certified results.
- 2) The NS-PIM solution applied to Biot's consolidation still possesses different convergence in displacement results and similar convergence in pore pressure results compared to the FEM solution. This property can be used to determine the computational errors of the solutions and get more accurate results. According to the results of this work, when the ERR1 for displacement is less than 0.5% and the ERR1 for pore pressure is less than 0.15%, the accuracy would be enough for general analysis.
- 3) The proposed method for estimating the computational error makes it possible to obtain accurate results with fewer 'remeshing works'. NS-PIM solution as one of the mesh free methods definitely makes the meshing and calculation for consolidation analysis easier and more efficient.

Thus, it is promising to apply the NS-PIM to the consolidation analysis. Also, more accurate and convincing results can be got based on the different convergence features between the FEM and NS-PIM solutions.

Meanwhile, it cannot be denied that the calculation of NS-PIM solution takes more time than that of the FEM solution, as the point interpolation for NS-PIM shape functions involves more nodes and procedures than that of the FEM solution. Although optimizations like node renumbering have been done in the solutions, more works are still necessary to be carried out to optimize the NS-PIM solution. Also, in further study, the feasibility of nonlinear, elastoplastic and 3D model can still be probed in the NS-PIM solution.

5 Acknowledgements

The support of the Fundamental Research Funds for the Central Universities (No. 2015B15114) and the Natural Science Foundation of China (No. 51009056) is gratefully acknowledged.

Reference

- [1] SM Gourvenec, C Vulpe, TG Murthy. A method for predicting the consolidated undrained bearing capacity of shallow foundations. *Geotechnique* 2014; 64: 215–225.
- [2] ZY Ai, CC Yi. 3-d consolidation analysis of layered soil with anisotropic permeability using analytical layer-element method. *Acta Mechanica Solida Sinica* 2013; 26(1): 62-70.
- [3] DV Griffiths, J Huang. One-dimensional consolidation theories for layered soil and coupled and uncoupled solutions by the finite-element method. *Géotechnique* 2010; 60: 709–713.
- [4] ZY Ai, YD Hu. Multi-dimensional consolidation of layered poroelastic materials with anisotropic permeability and compressible fluid and solid constituents. *Acta Geotech* 2015; 10: 263-273.
- [5] MA Biot. General theory of three-dimensional consolidation. *J. Appl. Phys* 1941; 12 : 155–164.
- [6] Zienkiewicz OC, Taylor RL. *The Finite Element Method* (5th edn). (V1: The basis), Butterworth-Heinemann: Oxford, 2000.
- [7] S Cen, C Li, S Rajendran, Z Hu. *Advances in finite element method*, Math. Probl. Eng. 2014; 2014: 0–3.
- [8] I M Smith, D V Griffiths, L Margetts. *Programming the finite element method*. John Wiley & Sons Ltd: United Kingdom, 2014 .

- [9] GR Liu, D Karamanlidis. Mesh Free Methods: Moving Beyond the Finite Element Method, *Appl. Mech. Rev* 2003; 56(2): B17-B18.
- [10] GR Liu, Y Li, KY Dai, MT Luan, W Xue. a Linearly Conforming Radial Point Interpolation Method for Solid Mechanics Problems. *Int. J. Comput. Methods* 2011; 3(4): 401–428.
- [11] GY Zhang, GR Liu, YY Wang, HT Huang, ZH Zhong, GY Li, X Han. A linearly conforming point interpolation method (LC-PIM) for three-dimensional elasticity problems. *Int. J. Numer. Methods Eng* 2007; 72 (13): 1524–1543.
- [12] J Cheng, XL Chang, SC Wu, GY Zhang. Certified solutions for hydraulic structures using the node-based smoothed point interpolation method (NS-PIM). *Int. J. Numer. Anal. Methods Geomech* 2009; 34 (15): 1560–1585.
- [13] GR Liu, YT Gu. A point interpolation method for two-dimensional solids. *Int. J. Numer. Methods Eng* 2001; 50(4): 937–951.
- [14] JG Wang, GR Liu. A point interpolation meshless method based on radial basis functions. *Int. J. Numer. Methods Eng* 2002; 54(11): 1623–1648.
- [15] Y Krongauz, T Belytschko. Enforcement of essential boundary conditions in meshless approximations using finite elements. *Comput. Methods Appl. Mech. Eng* 1996; 131(1-2): 133–145.
- [16] GR Liu, GY Zhang. Upper bound solution to elasticity problems: A unique property of the linearly conforming point interpolation method (LC-PIM). *Int. J. Numer. Methods Eng* 2008; 74(7): 1128–1161.
- [17] GY Zhang, GR Liu, TT Nguyen, CX Song, X Han, ZH Zhong, GY Li. The upper bound property for solid mechanics of the linearly conforming radial point interpolation method (LC-RPIM). *Int. J. Comput. Methods* 2011; 04(3): 521–541.
- [18] GY Zhang, GR Liu, Y Li. An efficient adaptive analysis procedure for certified solutions with exact bounds of strain energy for elasticity problems. *Finite Elem. Anal. Des* 2008; 44(14): 831–841.
- [19] JG Wang, GR Liu, YG Wu. A point interpolation method for simulating dissipation process of consolidation. *Comput. Methods Appl. Mech. Eng* 2001; 190(45): 5907–5922.
- [20] P Mira, M Pastor, T Li, X Liu. Failure problems in soils An enhanced strain coupled formulation with application. *Revue Française De Génie Civil* 2004; 8(5-6):735-759.
- [21] GR Liu, GY Zhang. Edge-Based Smoothed Point Interpolation Methods. *Int. J. Comput. Methods* 2011; 5(4): 621–646.
- [22] J Chen, C Wu, S Yoon. A stabilized conforming nodal integration for Galerkin mesh-free methods. *Int. J. Numer. Meth. Eng* 2001; 50(2): 435–466.
- [23] R Schiffman. Consolidation of soil under time-dependent loading and varying permeability. *Highway Research Board Proceedings* 1958; 37.